Wolf–Hirschhorn syndrome candidate 1 facilitates alveolar macrophage pyroptosis in sepsis-induced acute lung injury through NEK7-mediated NLRP3 inflammasome activation

Caixia Liu[1], Benlong Cai[1], Dan Li[2] and Yuan Yao[1]

Abstract

Sepsis is a complex clinical syndrome with high incidence and mortality. Acute lung injury (ALI) is a common complication of sepsis. At present, there is no effective therapeutic strategy to treat ALI. The SET domain–containing histone methyltransferase Wolf–Hirschhorn syndrome candidate 1 (WHSC1) regulates cancer progression, while its role in sepsis-induced ALI remains unclear. Thus, this study aimed to study the effect of WHSC1 on sepsis-induced ALI and to explore the potential mechanism of action. In the study, LPS treatment induced lung injury. WHSC1 was highly expressed in LPS-induced ALI. Knockdown of WHSC1 attenuated LPS-induced ALI and pyroptosis *in vivo*. Besides, knockdown of WHSC1 attenuated LPS-induced alveolar macrophage pyroptosis *in vitro*. Furthermore, NIMA-related kinase-7 (NEK7) expression could be regulated by WHSC1, and NEK7 bound to NLRP3 in alveolar macrophages. Moreover, WHSC1 regulated alveolar macrophage pyroptosis through modulating NEK7-mediated NLRP3 inflammasome activation. In conclusion, WHSC1 was highly expressed in LPS-induced ALI. WHSC1 facilitated alveolar macrophage pyroptosis in sepsis-induced ALI through NEK7-mediated NLRP3 inflammasome activation. WHSC1 may be a valuable target for the therapy of sepsis-induced ALI.

Keywords

Sepsis, acute lung injury, WHSC1, NEK7, NLRP3 inflammasome

Introduction

Sepsis is a complex clinical syndrome with a high clinical incidence rate and mortality rate.[1] Each year, approximately 25 million children suffer from sepsis, and an estimated three million neonates, children and adolescents die of sepsis globally.[2] A dys-regulated systemic inflammatory response usually accompanies sepsis, and the progress of the disease can cause sepsis shock and even multiple organ failure syndrome.[3] Therefore, sepsis is a significant threat to public health. Acute lung injury (ALI) is a common complication of sepsis and is characterised by an excessive inflammatory response and increased alveolar damage, lung permeability and protein-rich pulmonary oedema.[4] Although advanced progression has been made in ALI therapy, there is no effective therapeutic strategy to treat ALI.

Pyroptosis is a programmed cell death and is characterised by rapid plasma membrane rupture and pro-inflammatory cytokine production.[5,6] Pyroptosis is triggered by inflammasomes and is dependent on

[1]Department of Paediatrics, Taihe Hospital, Hubei University of Medicine, China
[2]Department of Pathology, Taihe Hospital, Hubei University of Medicine, China

Corresponding author:
Yuan Yao, Department of Paediatrics, Taihe Hospital, Hubei University of Medicine, No. 32, Renmin South Road, Shiyan City, Hubei Province, China.
Email: new_dc@163.com

caspase-1.[7,8] Activation of inflammasome-related inflammatory caspases promotes caspase-1 activation and gasdermin D (GSDMD) cleavage, thereby resulting in IL-1β and IL-18 maturation and pyroptosis.[7,8] At present, increasing evidence shows that pyroptosis is related to ALI.[9–11] For example, ghrelin alleviated ALI by regulating pyroptosis.[9] In diseases related to infection, pyroptosis is usually triggered in monocytes, macrophages and dendritic cells. A previous study showed that alveolar macrophage pyroptosis occurred in LPS-induced ALI.[12] Wang et al. reported that dihydromyricetin alleviated sepsis-induced ALI through inhibiting NLRP3 inflammasome-dependent pyroptosis.[5] Therefore, regulation of alveolar macrophage pyroptosis may be a promising strategy for sepsis-induced ALI therapy.

Wolf–Hirschhorn syndrome candidate 1 (WHSC1) is a SET domain–containing histone methyltransferase.[13,14] WHSC1 could regulate NIMA-related kinase-7 (NEK7) through H3K36me2 and then promote squamous cell carcinoma of the head and neck.[15] Besides, NEK7 has been demonstrated to interact with NLRP3 to modulate pyroptosis.[16] At present, the role of WHSC1 in ALI has not been reported. According to the above evidence, we speculated that WHSC1 might regulate pyroptosis via regulating NEK7, thereby modulating ALI.

Therefore, we investigated the effect of WHSC1 on sepsis-induced ALI using *in vivo* and *in vitro* models and studied whether NEK7 mediated the action of WHSC1 on ALI.

Methods

Animals

C57BL/6 male mice (8 wk old, 20–22 g) were obtained from Beijing Laboratory Animal Research Centre (Beijing, China). All mice were acclimatised for 7 d before use and had access to food and water *ad libitum*. To establish the sepsis-induced ALI model, mice were injected with 5 or 10 mg/kg LPS (cat. #L2880; Sigma–Aldrich, St. Louis, MO) intraperitoneally. The sham mice were injected with the same volume of vehicle. Besides, to establish the sepsis-induced ALI model with knockdown of WHSC1, mice were intratracheally injected with adenovirus (Ad) of shWHSC1 (Ad-shWHSC1; Genscript, Nanjing, China) 3 d before being injected with 10 mg/kg LPS intraperitoneally. All mice were euthanised 24 h after LPS injection. All protocols were performed to comply with national and international regulations and policies. The Committee of Animal Experimentation of Taihe Hospital permitted the animal protocols.

Hematoxylin and eosin stain

After mice were euthanised, lung tissues were collected, fixed using 10% formalin and embedded using paraffin. Then, the tissues were cut into 5 μm sections and dyed with hematoxylin and eosin (HE). The stained tissues were viewed under a light microscope and scored by two senior pathologists.

ELISA

After mice were euthanised, bronchoalveolar lavage fluid (BALF) was harvested and centrifuged at about 200 g for 10 min at 4°C to obtain supernatants. The levels of IL-18 (cat. #ab216165) and IL-1β (cat. #ab113344) in BALF were detected using commercial ELISA kits (Abcam, Cambridge, UK) following the manufacturer's procedures.

Lung wet/dry ratios

After mice were euthanised, the left lungs were excised to measure the wet mass. Subsequently, the samples were transferred to an oven for 72 h at 60°C. Then, the dry masses of samples were recorded, and the ratio of wet mass to dry mass was calculated.

Determination of protein expression in BALF

After mice were euthanised, BALF was harvested and centrifuged at about 200 g for 10 min at 4°C to obtain supernatants. The total protein levels in BALF were detected utilising a bicinchoninic acid (BCA) kit (cat. #BCA1; Sigma–Aldrich).

Quantitative RT-PCR

Total RNA was extracted utilising TRIzol (cat. #T9424; Sigma–Aldrich), and cDNA was produced by reverse transcription through employing a cDNA synthesis kit (cat. #11117831001; Sigma–Aldrich) in accordance with the manufacturer's procedures. Afterwards, cDNA was subjected to quantitative PCR assay using SYBR Green Master Mix (cat. #4309155; Thermo Fisher Scientific, Waltham, MA). The primers of WHSC1 were: F, 5′-ATTTAGC ATCAAGCAGAGTCCC-3′; R, 5′-CGCAGTTTGG CATCGTGT-3′.[17] The relative mRNA WHSC1 expression was analysed using the $2^{-\Delta\Delta Ct}$ method by normalising to β-actin.

Western blot

Lysates from tissues and cells were prepared using RIPA lysis buffer and were quantified using a BCA kit (cat. #BCA1; Sigma–Aldrich). Afterwards, lysates were resolved in SDS-PAGE to separate proteins and were then transferred to polyvinylidene fluoride membranes. The membranes were immersed in 5% skimmed milk to block for non-specific binding and labelled with anti-WHSC1 (1:2000; cat. #ab223694;

Abcam), NLRP3 (1:500; cat. #ab214185; Abcam), ASC (1:2000; cat. #ab175449; Abcam), caspase-1 p20 (1:1000; cat. #PA5-99390; Thermo Fisher Scientific), IL-18 (1:1000; cat. #ab191860; Abcam), IL-1β (1:1000; cat. #ab234437; Abcam), GSDMD FL (full length GSDMD; 1:1000; cat. #ab219800; Abcam), GSDMD CL (GSDMD-N terminal segment; 1:1000; cat. #10137S; Cell Signaling Technology, Danvers, MA), NEK7 (1:3000; cat. #ab133514; Abcam) and β-actin (1:5000; cat. #ab8227; Abcam) Abs at 4°C for 12 h. Afterwards, the membranes were incubated with IgG H&L (HRP; 1:5000; cat. #ab6728; Abcam) for 2 h at room temperature. β-Actin was designated as the internal control protein. Densitometry of bands was measured utilising the ECL Western Blotting Substrate (cat. #32132X3; Thermo Fisher Scientific).

Alveolar macrophage isolation

After mice were euthanised, BALF was harvested. The immunomagnetic separation system was employed to separate alveolar macrophages. Magnetic nanoparticle-conjugated anti-mouse Gr-1 (cat. #553129), anti-CD4 (cat. #561091), anti-CD8 (cat. #561093) and anti-CD45R/B220 (cat. #561880) Abs (BD Biosciences Pharmingen, San Diego, CA) were utilised to label and remove polymorphonuclear leucocytes and lymphocytes. The purity of macrophages in the remaining cells was > 98%. After the macrophages were harvested, cells were transfected with siRNA targeting WHSC1 (siWHSC1), siRNA targeting NEK7 (siNEK7) or NEK7 overexpression vector (Genscript) using Lipofectamine 3000 (cat. #L3000015; Thermo Fisher Scientific) and treated with 1 μg/ml LPS.

Co-immunoprecipitation

Alveolar macrophages were lysed using RIPA lysis buffer, and the protein content was quantified with a BCA kit (cat. #BCA1; Sigma–Aldrich). The lysates were then incubated with anti-NEK7 Ab (cat. #ab133514; Abcam) or anti-IgG Ab (cat. #ab190475; Abcam) with protein A/G agarose beads (cat. #sc-2003; Santa Cruz Biotechnology, Santa Cruz, CA) at 4°C overnight. Afterwards, the beads were harvested by centrifugation and washed. Finally, the precipitated proteins were eluted and subjected to Western blot.

Cell pyroptosis

Flow cytometry was conducted to determine macrophage cell pyroptosis. Cells were harvested and stained with Alexa Fluor 488-labelled anti-caspase-1 at 37°C for 1 h using the FAM-FLICA Caspase Assay Kit (cat. #98; ImmunoChemistry Technology, Bloomington, MN), following by dying with propidium iodide (PI) for 5 min. Subsequently, cells were subjected to flow cytometry (BD FACSCalibur, Franklin Lakes, NJ). Cells positive for caspase-1 and PI were considered as pyroptotic cells.

Determination of caspase-1 activity

The Caspase-1 Colorimetric Assay Kit (cat. #K111; BioVision, Milpitas, CA) was utilised to detect caspase-1 activity in tissues and cells according to the manufacturer's protocols after lung tissues or cells were collected. Absorbance at 450 nm was recorded using a microplate reader.

Immunofluorescence

To perform immunofluorescence staining, macrophages were fixed for 30 min by 4% paraformaldehyde, penetrated for 1 h utilising 0.3% Triton X-100 and blocked for 30 min using 5% bovine albumin. Afterwards, cells were probed with anti-caspase-1 Ab (cat. #PA5-99390; Thermo Fisher Scientific) and anti-GSDMD-CL Ab (cat. #ER1901-37; HUABIO, Hangzhou, China) overnight at 4°C. Subsequently, cells were incubated with goat anti-rabbit Alexa Fluor 594 secondary Ab (cat. #ab150080; Abcam) and donkey Anti-Rabbit Alexa Fluor 488 secondary Ab (cat. #ab150073; Abcam) for 1 h. The nuclei of macrophages were dyed with DAPI for 5 min. Finally, the macrophages were observed under the confocal microscope (Zeiss, Jena, Germany).

Statistical analysis

All data are presented as the mean ± SD and processed by using IBM SPSS Statistics for Windows v22.0 (IBM Corp., Armonk, NY). Student's t-test and one-way ANOVA with least significant difference post hoc test were used to compare group differences. The criterion of difference statistically significant was $P < 0.05$.

Results

WHSC1 was up-regulated in LPS-induced ALI

To investigate the role of WHSC1 in ALI, the ALI mice model was established by intraperitoneally injecting with 5 or 10 mg/kg LPS. HE staining was conducted to determine lung tissue injury. It was observed that alveolar became small and irregular, the alveolar wall thickened and inflammation cells infiltrated the lung tissues of mice treated with LPS (Figure 1a). The lung injury score was significantly increased in LPS-induced mice compared to sham mice ($P < 0.001$; Figure 1b). Besides, the levels of IL-18 and IL-1β in BALF were elevated in LPS-induced
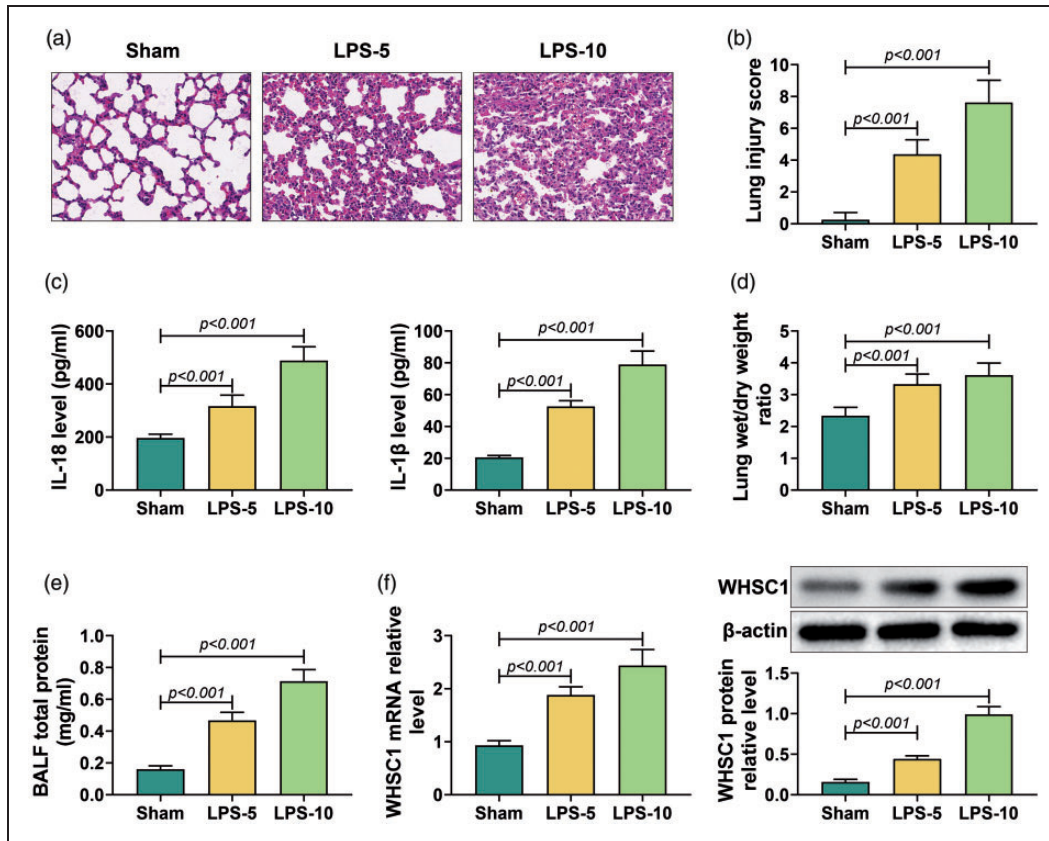
Figure 1. Wolf–Hirschhorn syndrome candidate 1 (WHSC1) was up-regulated in LPS-induced acute lung injury (ALI). (a) Hematoxylin and eosin (HE) stain was conducted to assess lung tissue damage in mice treated with 5 or 10 mg/kg LPS. (b) The lung injury score was determined to evaluate lung injury in mice treated with LPS. (c) Levels of IL-18 and IL-1β in bronchoalveolar lavage fluid (BALF) were detected by ELISA assay. (d) The lung wet/dry mass ratio of lung tissue was measured in mice treated with LPS. (e) The level of BALF total protein was determined in mice treated with LPS. (f) The mRNA and protein levels of WHSC1 in alveolar macrophages of mice treated with LPS were detected by quantitative RT-PCR and Western blot.

mice ($P < 0.001$; Figure 1c). In addition, LPS treatment also increased the lung wet/dry mass ratio and total protein level in BALF ($P < 0.001$; Figure 1d and e). Furthermore, WHSC1 expression in alveolar macrophages of ALI mice was determined. Results showed that the mRNA and protein levels of WHSC1 were remarkably up-regulated in alveolar macrophages of LPS-induced ALI mice ($P < 0.001$; Figure 1f). Therefore, the ALI mice model was successfully established, and WHSC1 was highly expressed in LPS-induced ALI.

Knockdown of WHSC1 attenuated LPS-induced ALI

To determine the action of WHSC1 on ALI, Ad-shWHSC1 was introduced into mice before injecting with 10 mg/kg LPS. The knockdown efficiency of Ad-shWHSC1 was confirmed by quantitative RT-PCR and Western blot. Results showed that the mRNA and protein levels of WHSC1 in alveolar macrophages were significantly inhibited by Ad-shWHSC1 ($P < 0.001$;

Figure 2a). Subsequently, the effect of WHSC1 knockdown on LPS-induced ALI was explored. It was observed that the lung tissue damage induced by LPS was attenuated by knockdown of WHSC1 (Figure 2b). LPS stimulation increased the lung injury score, which was decreased by knockdown of WHSC1 ($P < 0.001$; Figure 2c). Besides, the elevated levels of IL-18 and IL-1β in LPS-induced ALI mice were suppressed by knockdown of WHSC1 ($P < 0.001$; Figure 2d). Furthermore, the increased lung wet/dry mass ratio caused by LPS was inhibited by knockdown of WHSC1 ($P < 0.001$; Figure 2e). Knockdown of WHSC1 also suppressed the LPS-induced BALF total protein levels ($P < 0.001$; Figure 2f). Thus, knockdown of WHSC1 attenuated LPS-induced ALI.

Knockdown of WHSC1 attenuated LPS-induced pyroptosis

To understand better the role of WHSC1 in ALI, the effects of WHSC1 knockdown on alveolar macrophage
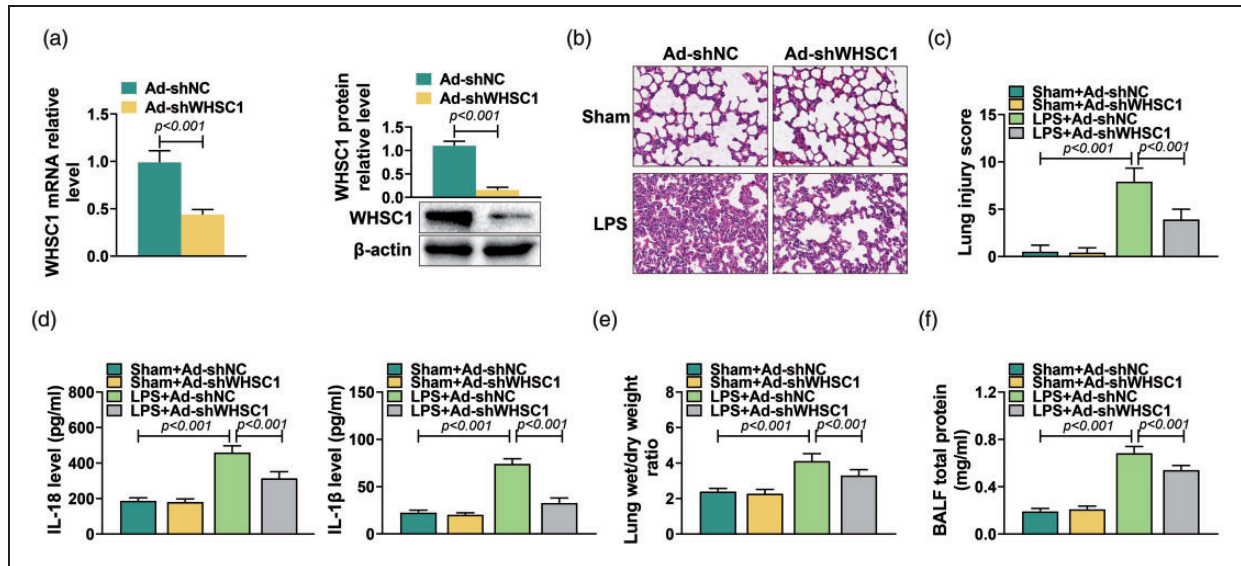
Figure 2. Knockdown of WHSC1 attenuated LPS-induced ALI. (a) The mRNA and protein levels of WHSC1 were detected by quantitative RT-PCR and Western blot in alveolar macrophages of mice introduced into Ad-shWHSC1 and treated with 10 mg/kg LPS. (b) The lung tissue damage in mice introduced into Ad-shWHSC1 and treated with 10 mg/kg LPS was determined by HE stain. (c) The lung injury score was determined to evaluate lung injury in mice introduced into Ad-shWHSC1 and treated with 10 mg/kg LPS. (d) The levels of IL-18 and IL-1β in BALF of mice introduced into Ad-shWHSC1 and treated with 10 mg/kg LPS were detected by ELISA assay. (e) The lung wet/dry mass ratio of lung tissues in mice introduced into Ad-shWHSC1 and treated with 10 mg/kg LPS was determined. (f) The BALF total protein level was determined in mice introduced into Ad-shWHSC1 and treated with 10 mg/kg LPS.

pyroptosis were explored. Western blot was conducted to determine the activation of NLRP3 inflammasome hallmarks, including NLRP3, ASC, caspase-1 p20, IL-18, IL-1β, GSDMD FL and GSDMD CL in alveolar macrophages of ALI mice. Results showed that the levels of NLRP3, ASC, caspase-1 p20, IL-18, IL-1β and GSDMD CL were promoted by LPS ($P < 0.001$), which were inhibited by knockdown of WHSC1 except for ASC in alveolar macrophages of ALI mice ($P < 0.001$; Figure 3a). In addition, LPS stimulation did not affect GSDMD FL expression, while knockdown of WHSC1 increased the expression of GSDMD FL ($P < 0.001$; Figure 3a). Furthermore, results revealed that the activity of caspase-1 was induced by LPS, which was suppressed by knockdown of WHSC1 ($P < 0.001$; Figure 3b). Hence, knockdown of WHSC1 attenuated LPS-induced alveolar macrophage pyroptosis.

Knockdown of WHSC1 attenuated LPS-induced alveolar macrophage pyroptosis

To investigate further the effect of WHSC1 on macrophage pyroptosis, the alveolar macrophages were isolated from mice and transfected into siRNA targeting WHSC1. The transfection efficiency of siRNA targeting WHSC1 was confirmed by Western blot ($P < 0.001$; Figure 4a). Knockdown of WHSC1 suppressed the LPS-induced increase of NLRP3, caspase-1 p20, IL-18, IL-1β and GSDMD CL protein levels in macrophages

($P < 0.001$; Figure 4b). However, knockdown of WHSC1 did not affect the increased ASC level induced by LPS in macrophages (Figure 4b). Besides, LPS stimulation did not affect GSDMD FL expression, while knockdown of WHSC1 increased the expression of GSDMD FL in macrophages ($P < 0.001$; Figure 4b). Furthermore, the increased activity of caspase-1 induced by LPS was inhibited by the knockdown of WHSC1 ($P < 0.001$; Figure 4c). Moreover, flow cytometry revealed the pyroptosis proportion of macrophages was induced by LPS but was reversed by knockdown of WHSC1 ($P < 0.001$; Figure 4d). Immunofluorescence results also proved that knockdown of WHSC1 suppressed the LPS-induced increase of caspase-1 and GSDMD CL in macrophages ($P < 0.001$; Figure 4f). Therefore, knockdown of WHSC1 attenuated LPS-induced alveolar macrophage pyroptosis.

WHSC1 regulated alveolar macrophage pyroptosis through modulating NEK7 expression

A previous study proved that WHSC1 could regulate the expression of NEK7. We inferred that WHSC1 might regulate alveolar macrophage pyroptosis through modulating NEK7 expression. Therefore, the expression of NEK7 was explored in alveolar macrophages after the knockdown of WHSC1. Results showed that the mRNA and protein expression of NEK7 in alveolar macrophages was induced by LPS,
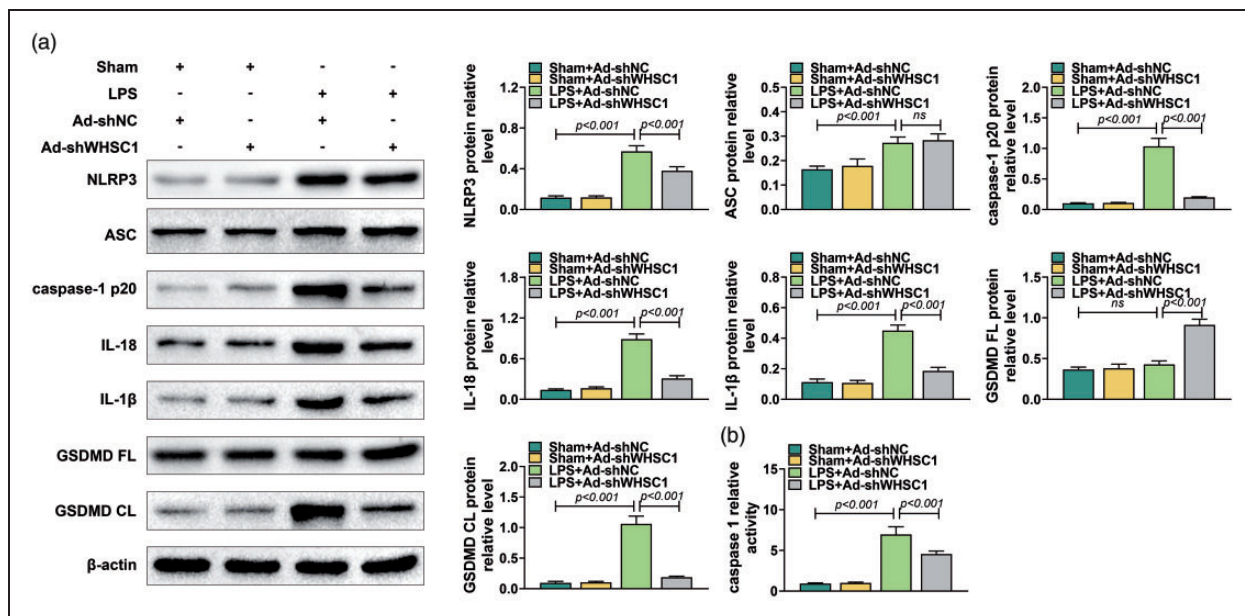
Figure 3. Knockdown of WHSC1 attenuated LPS-induced pyroptosis. (a) The protein levels of NLRP3, ASC, caspase-1 p20, IL-18, IL-1β, GSDMD FL and GSDMD CL in alveolar macrophages of mice introduced into Ad-shWHSC1 and treated with 10 mg/kg LPS were detected using Western blot. (b) The activity of caspase-1 in the alveolar macrophage of mice introduced into Ad-shWHSC1 and treated with 10 mg/kg LPS was determined. Ns: $P > 0.05$.

which was decreased by knockdown of WHSC1 ($P < 0.001$; Figure 5a). In addition, the expression of NEK7 in alveolar macrophages of LPS-induced ALI mice was also increased but was inhibited by knockdown of WHSC1 ($P < 0.001$; Figure 5b). Besides, co-immunoprecipitation assay revealed that NEK7 could bind to NLRP3 (Figure 5c). Furthermore, Western blot found that knockdown of NEK7 had no effect on WHSC1 and ASC expression, but significantly inhibited the expression level of NEK7, NLRP3, caspase-1 p20, IL-18, IL-1β and GSDMD CL and increased the expression of GSDMD FL ($P < 0.001$; Figure 5d). The inhibitory effects of WHSC1 knockdown on the expression levels of NEK7, NLRP3, caspase-1 p20, IL-18, IL-1β and GSDMD CL were strengthened by NEK7 knockdown except for IL-18 ($P < 0.001$; Figure 5d). Similarly, immunofluorescence results found that knockdown of NEK7 strengthened the inhibitory effects of WHSC1 knockdown on the expression of caspase-1 and GSDMD CL (Figure 6a). Moreover, the inhibitory effects of WHSC1 knockdown the caspase-1 activity and pyroptosis proportion of macrophages were further fastened by NEK7 knockdown ($P < 0.05$; Figure 6b–d).

To investigate further whether WHSC1 regulated alveolar macrophage pyroptosis through modulating NEK7 expression, NEK7 overexpression vector and siRNA targeting WHSC1 were co-transfected into LPS-induced macrophages. Results showed that NEK7 overexpression vector significantly increased

the protein level of NEK7 ($P < 0.001$; Figure 7a). Besides, overexpressed NEK7 increased the protein levels of NLRP3, caspase-1 p20, IL-18, IL-1β and GSDMD CL in macrophages transfected with siRNA targeting WHSC1 and induced by LPS ($P < 0.05$; Figure 7b). The activity of caspase-1 also was increased by overexpressed NEK7 ($P < 0.001$; Figure 7c). Furthermore, immunofluorescence results showed that overexpression of NEK7 increased the expressions of caspase-1 and GSDMD CL in macrophages transfected with siRNA targeting WHSC1 and induced by LPS ($P < 0.05$; Figure 7d). Taken together, WHSC1 regulated alveolar macrophage pyroptosis through modulating NEK7 expression.

Discussion

Sepsis is a severe clinical syndrome with a high incidence rate and mortality rate and accompanied by dysregulated systemic inflammatory response multiple organ failure syndrome[1,3] ALI is a common complication of sepsis, which is a clinical challenge.[4] Therefore, it is essential to explore an effective therapeutic strategy for sepsis-induced ALI. The SET domain–containing histone methyltransferase WHSC1 has been proved to regulate cancer progression,[18,19] while its role in ALI remains unclear. Hence, we investigated the action of WHSC1 on sepsis-induced ALI in this study and found that WHSC1 promoted alveolar macrophage
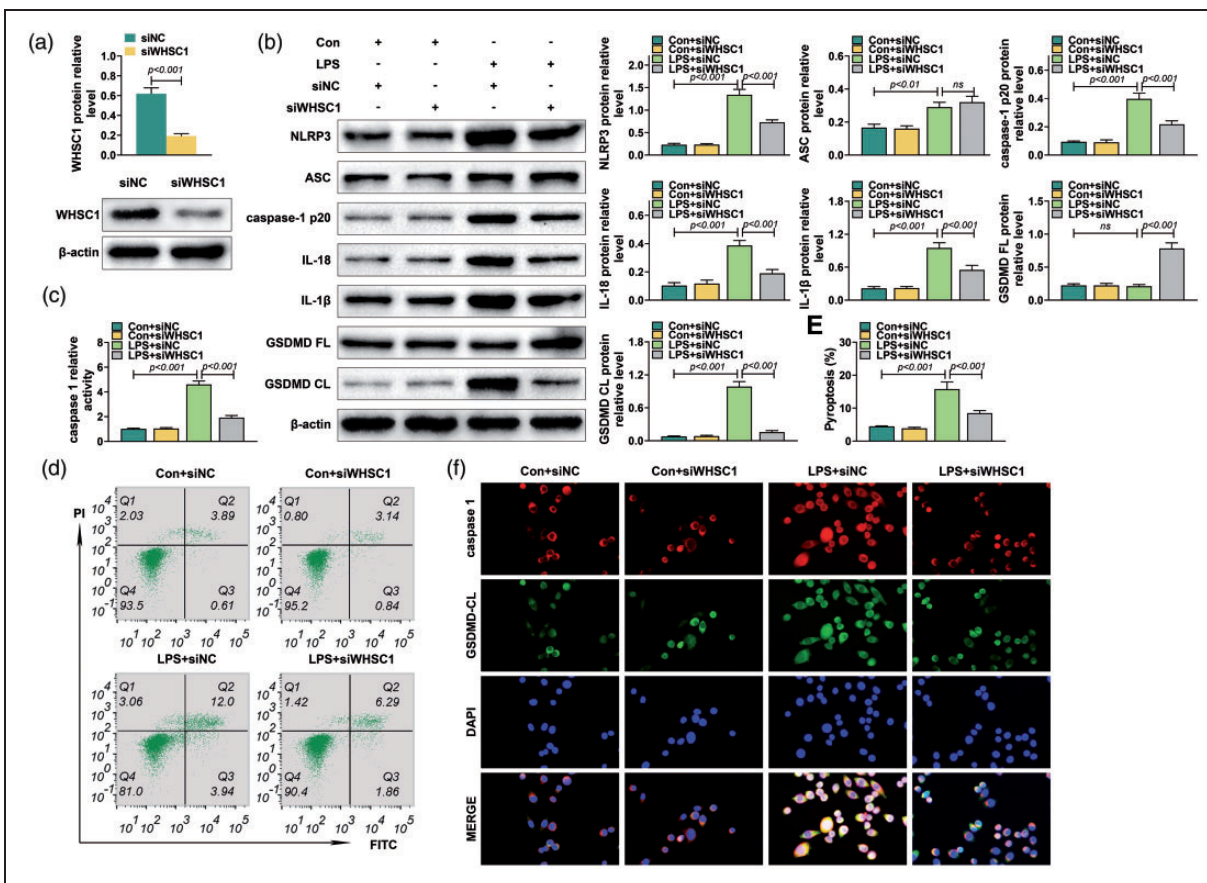
Figure 4. Knockdown of WHSC1 attenuated LPS-induced alveolar macrophage pyroptosis. (a) The protein level of WHSC1 was determined using Western blot in alveolar macrophages transfected with siRNA targeting WHSC1. (b) The protein levels of NLRP3, ASC, caspase-1 p20, IL-18, IL-1β, GSDMD FL and GSDMD CL were determined using Western blot in alveolar macrophages transfected with siRNA targeting WHSC1 and treated with 1 µg/ml LPS. (c) The activity of caspase-1 in alveolar macrophages transfected with siRNA targeting WHSC1 and treated with 1 µg/ml LPS was determined. (d) The pyroptosis proportion of macrophages transfected with siRNA targeting WHSC1 and treated with 1 µg/ml LPS was assessed by flow cytometry. (f) The expressions of caspase-1 and GSDMD CL in alveolar macrophages transfected with siRNA targeting WHSC1 and treated with 1 µg/ml LPS were determined by immunofluorescence. Ns: $P > 0.05$.

pyroptosis in sepsis-induced ALI through NEK7-mediated NLRP3 inflammasome activation.

To imitate sepsis-induced ALI, mice were intraperitoneally injected with LPS. LPS is a vital component of most Gram-negative bacteria's outer membrane, which can be captured by an Ag-presenting cell and causes an inflammatory response after bacteria invade the body.[20] An intraperitoneal injection of LPS can induce systemic inflammation in mice, which is similar to many of the initial clinical features of sepsis.[21] Therefore, LPS was used to imitate sepsis-induced ALI. After being induced by LPS, lung tissue damage occurred in the study. Besides, IL-18 and IL-1β in BALF, lung wet/dry mass ratio and total protein level in BALF were increased in mice with sepsis induced by LPS. These findings show that LPS induced lung tissue damage, inflammatory response and alveolar–capillary barrier dysfunction in mice. Similar

results have been reported in previous studies.[22,23] These results indicated that the ALI mice model was successfully established.

The SET domain–containing histone methyltransferase WHSC1 is a vital regulator in cancer progression.[18,19] However, the action of WHSC1 in ALI remains unclear. Alveolar macrophages are critical leucocytes and account for 90% of the cells in BALF.[24,25] Alveolar macrophages can function as guardians for the alveolar–blood interface against airborne particles and microbes.[25] After being activated, alveolar macrophages can recruit neutrophils and circulating macrophages to the injury site though releasing inflammatory mediators, and these cells further induce inflammatory events.[26] Therefore, alveolar macrophages are critical in the development of ALI. and these cells were selected to investigate the role of WHSC1 in ALI in this study. Hence, the expression of WHSC1 in alveolar
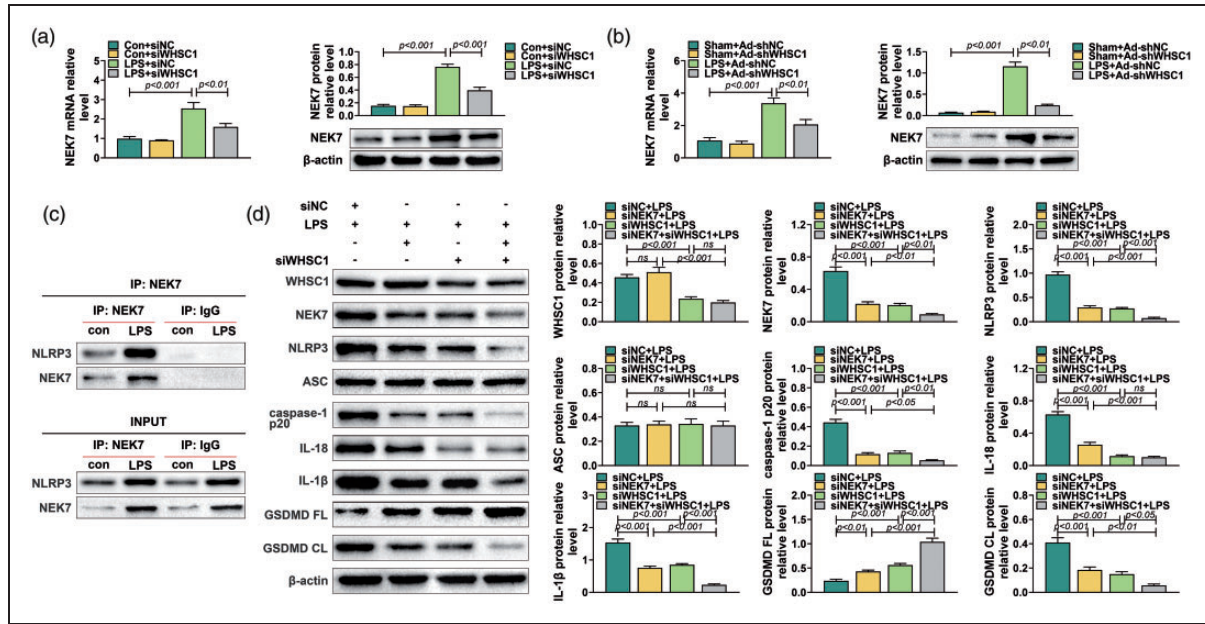
Figure 5. Knockdown of NEK7 enhanced the inhibitory effect of WHSC1 silencing on LPS-induced alveolar macrophage pyroptosis. (a) The expression level of NEK7 was determined using quantitative RT-PCR and Western blot in alveolar macrophages transfected with siRNA targeting WHSC1 and treated with 1 µg/ml LPS. (b) The expression level of NEK7 was determined using quantitative RT-PCR and Western blot in alveolar macrophages of mice introduced into Ad-shWHSC1 and treated with 10 mg/kg LPS. (c) A co-immunoprecipitation assay was performed to explore the relationship between NEK7 and NLRP3. (d) The protein levels of WHSC1, NEK7, NLRP3, ASC, caspase-1 p20, IL-18, IL-1β, GSDMD FL and GSDMD CL were determined using Western blot in alveolar macrophages transfected with siRNAs targeting WHSC1 and NEK7 and treated with 1 µg/ml LPS. Ns: $P > 0.05$.
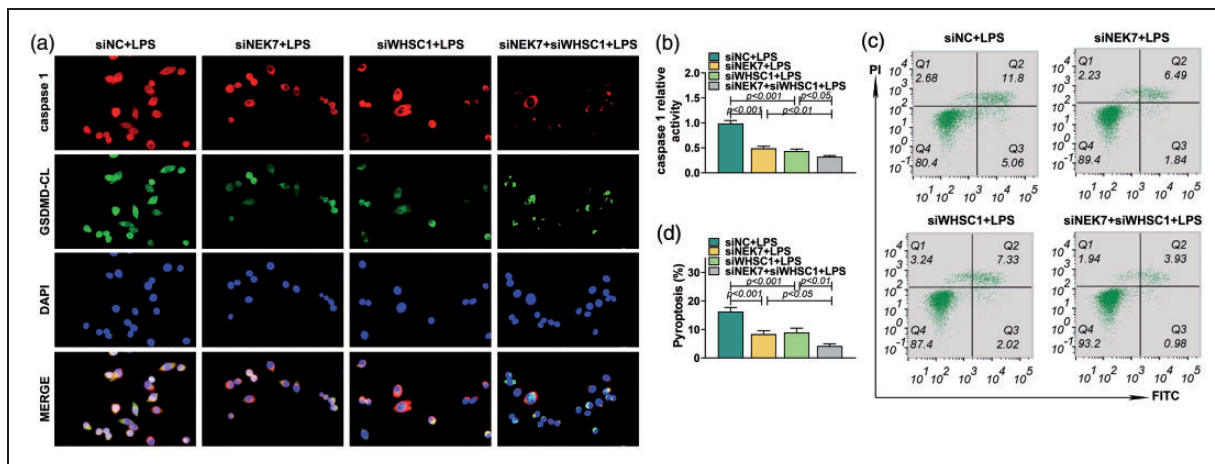

Figure 6. The effect of WHSC1 and NEK7 on alveolar macrophage pyroptosis. (a) The expressions of caspase-1 and GSDMD CL in alveolar macrophages transfected with siRNAs targeting WHSC1 and NEK7 and treated with 1 µg/ml LPS were detected using immunofluorescence. (b) The activity of caspase-1 in alveolar macrophages was determined in alveolar macrophages transfected with siRNAs targeting WHSC1 and NEK7 and treated with 1 µg/ml LPS. (c) The pyroptosis of macrophages in alveolar macrophages transfected with siRNAs targeting WHSC1 and NEK7 and treated with 1 µg/ml LPS was assessed by flow cytometry. (d) The pyroptosis proportion of macrophages in alveolar macrophages transfected with siRNAs targeting WHSC1 and NEK7 and treated with 1 µg/ml LPS is presented.

macrophages was first detected after ALI was induced by LPS, and highly expressed WHSC1 was presented in LPS-induced ALI. The aberrant expression of WHSC1 hinted that it might be involved in the regulation of ALI. Therefore, we determined the effect of WHSC1 on ALI *in vivo*. The results indicated that knockdown of WHSC1 attenuated LPS-induced lung tissue damage, inflammatory response and alveolar–capillary
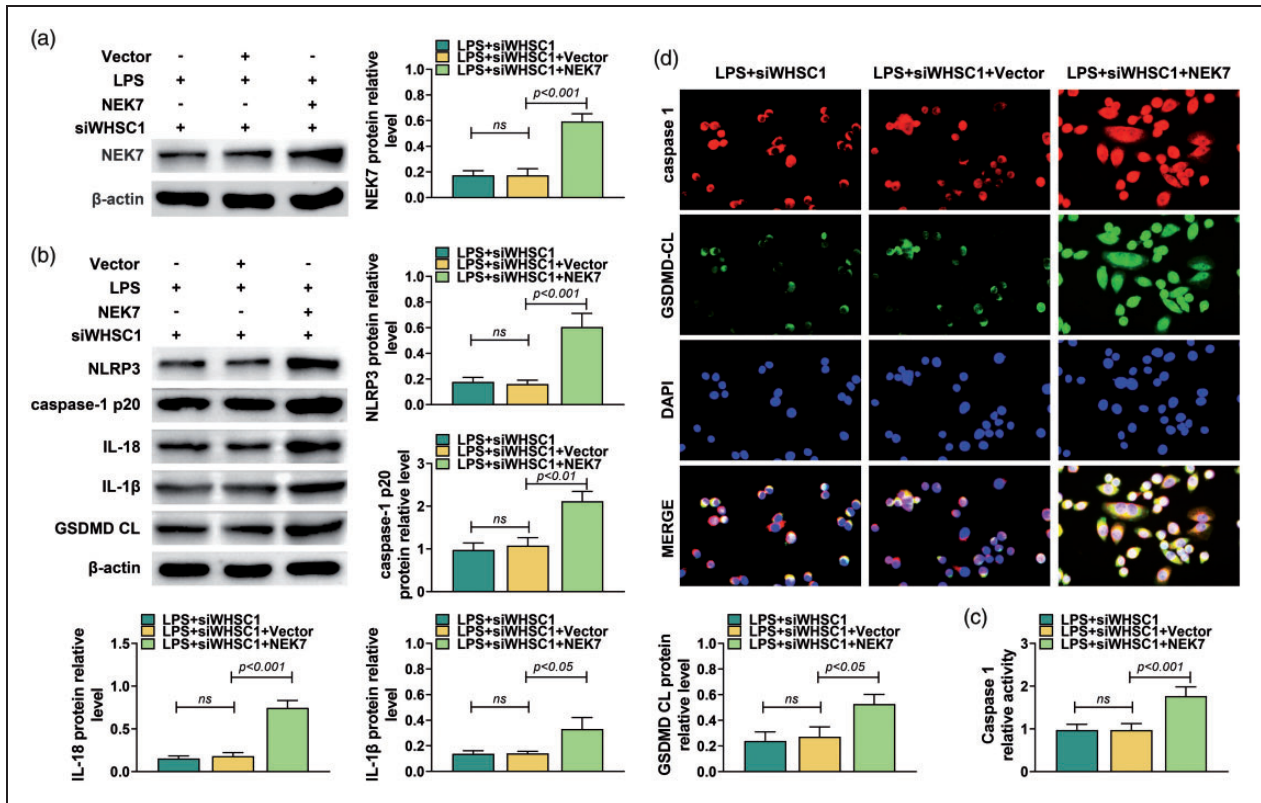
Figure 7. Enforced NEK7 reversed the inhibitory effect of WHSC1 silencing on LPS-induced alveolar macrophage pyroptosis. (a) The expression level of NEK7 was determined using Western blot in alveolar macrophages co-transfected with NEK7A overexpression vector and siRNAs targeting WHSC1 and treated with 10 mg/kg LPS. (b) The protein levels of WHSC1, NEK7, NLRP3, ASC, caspase-1 p20, IL-18, IL-1β and GSDMD CL were determined using Western blot in alveolar macrophages co-transfected with NEK7A overexpression vector and siRNAs targeting WHSC1 and treated with 10 mg/kg LPS. (c) The activity of caspase-1 in alveolar macrophage was determined in alveolar macrophages co-transfected with NEK7A overexpression vector and siRNAs targeting WHSC1 and treated with 10 mg/kg LPS. (d) The expressions of caspase-1 and GSDMD CL in alveolar macrophages co-transfected with NEK7A overexpression vector and siRNAs targeting WHSC1 and treated with 10 mg/kg LPS were detected using immuno-fluorescence. Ns: $P > 0.05$.

barrier dysfunction. Besides, the action of WHSC1 on pyroptosis was explored *in vivo* and *in vitro*. Accumulating evidence on pyroptosis revealed that activated NLRP3 could form a protein complex NLRP3 inflammasome with ASC and pro-caspase-1.[27] Active caspase-1 cleaved GSDMD within a linker between its N-terminal and C-terminal domains to initiate pyroptosis and stimulate IL-1β and IL-18, causing the release of these active cytokines from pyroptotic macrophages.[27] Therefore, the hallmarks of activation of NLRP3 inflammasome, including NLRP3, ASC, caspase-1 p20, IL-18, IL-1β, GSDMD FL and GSDMD CL, in alveolar macrophages were detected to indicate the effect of WHSC1 on alveolar macrophage pyroptosis. Both *in vivo* and *in vitro* results revealed that the knockdown of WHSC1 attenuated LPS-induced alveolar macrophage pyroptosis. Therefore, the knockdown of WHSC1 attenuated LPS-induced ALI and pyroptosis. Given that WHSC1 was elevated in LPS-induced

alveolar macrophages, WHSC1 could induce alveolar macrophage pyroptosis in sepsis-induced ALI. This study is the first to reveal the effects of WHSC1 on LPS-induced ALI.

A previous study reported that WHSC1 could regulate NEK7 through H3K36me2.[15] Besides, NEK7 could interact with NLRP3 to modulate pyroptosis.[16] Therefore, we inferred that WHSC1 might regulate pyroptosis in LPS-induced ALI through regulating NEK7. Thus, the regulating role of WHSC1 on NEK7 expression in alveolar macrophages was detected. Results showed that the knockdown of WHSC1 inhibited the expression of NEK7 induced by LPS. The result was consistent with a previous study.[15] Saloura et al. also proved that down-regulation of WHSC1 decreased the expression of NEK7.[15] Besides, a co-immunoprecipitation assay revealed that NEK7 could bind to NLRP3, which was similar to previous studies.[16,28] Chen et al. reported that NEK7 interacted with NLRP3 to modulate pyroptosis in

inflammatory bowel disease.[16] He et al. found that NEK7 was an essential mediator of NLRP3 activation downstream of potassium efflux.[28]

Given the relationship among WHSC1, NEK7 and NLRP3, we speculated that WHSC1 might regulate alveolar macrophage pyroptosis in LPS-induced ALI through NEK7-mediated NLRP3 inflammasome activation. Afterwards, the conjecture was confirmed in LPS-induced alveolar macrophages. These findings suggested that there was one such regulatory pathway in alveolar macrophage pyroptosis in LPS-induced ALI: elevated WHSC1 in alveolar macrophages of LPS-induced ALI increased the expression of NEK7, which bound to NLRP3 and activated NLRP3. Activated NLRP3 formed a protein complex NLRP3 inflammasome with ASC and pro-caspase-1.[27] Active caspase-1 could cleave GSDMD and stimulate IL-1β and IL-18, causing the release of these active cytokines from pyroptotic macrophages.[27] Therefore, WHSC1 modulated alveolar macrophage pyroptosis in LPS-induced ALI through regulating NEK7-mediated NLRP3 inflammasome activation.

A limitation of this study was that the underlying mechanism of WHSC1 on regulating NEK7 expression in LPS-induced ALI was not investigated. The problem will be explored in a future study.

Conclusion

WHSC1 was highly expressed in LPS-induced ALI. WHSC1 facilitated alveolar macrophage pyroptosis in sepsis-induced ALI through NEK7-mediated NLRP3 inflammasome activation. WHSC1 may be a valuable target for the therapy of sepsis-induced ALI.

Declaration of conflicting interests

Funding

ORCID iD

Yuan Yao https://orcid.org/0000-0002-3045-5765

References

1. Iskander KN, Osuchowski MF, Stearns-Kurosawa DJ, et al. Sepsis: multiple abnormalities, heterogeneous responses, and evolving understanding. *Physiol Rev* 2013; 93: 1247–1288.

2. Giannoni E and Schlapbach LJ. Sepsis in neonates and children. *Front Pediatr* 2020; 8: 621663.

3. Caraballo C and Jaimes F. Focus: Death: Organ Dysfunction in Sepsis: An Ominous Trajectory From Infection To Death. *The Yale Journal of Biology and Medicine*. 2019; 92: 629.

4. Li J, Liu L, Zhou X, et al. Melatonin attenuates sepsis-induced acute lung injury through improvement of epithelial sodium channel-mediated alveolar fluid clearance via activation of SIRT1/SGK1/Nedd4-2 signaling pathway. *Front Pharmacol* 2020; 11: 2004.

5. Wang Y-C, Liu Q-X, Zheng Q, et al. Dihydromyricetin alleviates sepsis-induced acute lung injury through inhibiting NLRP3 inflammasome-dependent pyroptosis in mice model. *Inflammation* 2019; 42: 1301–1310.

6. Bergsbaken T, Fink SL and Cookson BT. Pyroptosis: host cell death and inflammation. *Nat Rev Microbiol* 2009; 7: 99–109.

7. Sun L, Ma W, Gao W, et al. Propofol directly induces caspase-1-dependent macrophage pyroptosis through the NLRP3-ASC inflammasome. *Cell Death Dis* 2019; 10: 542.

8. He W-T ,Wan H, Hu L, et al. Gasdermin D is an executor of pyroptosis and required for interleukin-1β secretion. *Cell Res* 2015; 25: 1285–1298.

9. Shao X-F, Li B, Shen J, et al. Ghrelin alleviates traumatic brain injury-induced acute lung injury through pyroptosis/NF-κB pathway. *Int Immunopharmacol* 2020; 79: 106175.

10. Zeng Y, Qin Q, Li K, et al. PKR suppress NLRP3-pyroptosis pathway in lipopolysaccharide-induced acute lung injury model of mice. *Biochem Biophys Res Commun* 2019; 519: 8–14.

11. Wu X-B, Sun H-Y, Luo Z-L, et al. Plasma-derived exosomes contribute to pancreatitis-associated lung injury by triggering NLRP3-dependent pyroptosis in alveolar macrophages. *Biochim Biophys Acta Mol Basis Dis* 2020; 1866: 165685.

12. Wu D, Pan P, Su X, et al. Interferon regulatory factor-1 mediates alveolar macrophage pyroptosis during LPS-induced acute lung injury in mice. *Shock* 2016; 46: 329–338.

13. Stec I, Wright TJ, Van Ommen G-JB, et al. WHSC1, a 90 kb SET domain-containing gene, expressed in early development and homologous to a *Drosophila* dysmorphy gene maps in the Wolf–Hirschhorn syndrome critical region and is fused to IgH in t (1; 14) multiple myeloma. *Hum Mol Genet* 1998; 7: 1071–1082.

14. Kojima M, Sone K, Oda K, et al. The histone methyltransferase WHSC1 is regulated by EZH2 and is important for ovarian clear cell carcinoma cell proliferation. *BMC Cancer* 2019; 19: 1–9.

15. Saloura V, Cho H-S, Kiyotani K, et al. WHSC1 promotes oncogenesis through regulation of NIMA-related kinase-7 in squamous cell carcinoma of the head and neck. *Mol Cancer Res* 2015; 13: 293–304.

16. Chen X, Liu G, Yuan Y, et al. NEK7 interacts with NLRP3 to modulate the pyroptosis in inflammatory bowel disease via NF-κB signaling. *Cell Death Dis* 2019; 10: 1–12.

17. Wu J, Luo M, Duan Z, et al. WHSC1 acts as a prognostic indicator and functions as an oncogene in cervical cancer. *Onco Targets Ther* 2019; 12: 4683.

18. Li N, Xue W, Yuan H, et al. AKT-mediated stabilization of histone methyltransferase WHSC1 promotes prostate cancer metastasis. *J Clin Invest* 2017; 127: 1284–1302.

19. Yin Z, Sun Y, Ge S, et al. Epigenetic activation of WHSC1 functions as an oncogene and is associated with poor prognosis in cervical cancer. *Oncol Rep* 2017; 37: 2286–2294.

20. Wang X and Quinn PJ. Endotoxins: lipopolysaccharides of Gram-negative bacteria. *Subcell Biochem* 2010; 53: 3–25.

21. Lee H-H, Shin J-S, Lee W-S, et al. Biflorin, isolated from the flower buds of *Syzygium aromaticum* L., suppresses LPS-induced inflammatory mediators via STAT1 inactivation in macrophages and protects mice from endotoxin shock. *J Nat Prod* 2016; 79: 711–720.

22. Zhang Y, Huang T, Jiang L, et al. MCP-induced protein 1 attenuates sepsis-induced acute lung injury by modulating macrophage polarization via the JNK/c-Myc pathway. *Int Immunopharmacol* 2019; 75: 105741.

23. Zhang E, Wang J, Chen Q, et al. Artesunate ameliorates sepsis-induced acute lung injury by activating the mTOR/AKT/PI3K axis. *Gene* 2020; 759: 144969.

24. Ding H, Yang J, Chen L, et al. Memantine alleviates acute lung injury via inhibiting macrophage pyroptosis. *Shock*. Epub ahead of print 13 April 2021. DOI: 10.1097/SHK.0000000000001790.

25. Wu D, Pan P, Su X, et al. Interferon regulatory factor-1 mediates alveolar macrophage pyroptosis during LPS-induced acute lung injury in mice. *Shock* 2016; 46: 329–338.

26. Zheng H, Liang W, He W, et al. Ghrelin attenuates sepsis-induced acute lung injury by inhibiting the NF-κB, iNOS, and Akt signaling in alveolar macrophages. *Am J Physiol Lung Cell Mol Physiol* 2019; 317: L381–L391.

27. Li D, Ren W, Jiang Z, et al. Regulation of the NLRP3 inflammasome and macrophage pyroptosis by the p38 MAPK signaling pathway in a mouse model of acute lung injury. *Mol Med Rep* 2018; 18: 4399–4409.

28. He Y, Zeng MY, Yang D, et al. NEK7 is an essential mediator of NLRP3 activation downstream of potassium efflux. *Nature* 2016; 530: 354–357.